

Experimental Study of Energy Harvesting using a Self-Powered SSHI Interface Circuit

Action Nechibvute^{1*}, Pearson Luhanga² and Albert Chawanda¹

¹Physics Department, Midlands State University, P/Bag 9055, Gweru, Zimbabwe

²Physics Department, University of Botswana, P/Bag 0022, Gaborone, Botswana

ABSTRACT

The harvesting of energy from a vibrating structure using a piezoelectric bimorph transducer and a simple synchronised switching circuit is investigated experimentally. The switching circuit employed is a parallel synchronized switch harvesting on inductor (SSHI) interface that employs a self-powered electronic circuit breaker. The experimental results show that for the piezoelectric bimorph transducer used, the self-powered SSHI circuit can harvest up to 197 % more power compared to the standard energy harvesting (SEH) interface circuit. While the self-powered SSHI circuit evidently enhances the power harvested by a piezoelectric transducer, the experimental results show that at very low excitation levels the self-powered SSHI does not always outperform the standard circuit. This observation is seldom reported in literature on energy harvesting using nonlinear techniques. The results also suggest that as the excitation level increases, the performance of self-powered SSHI gets more beneficial compared to the SEH interface.

Keywords: *Synchronised switching circuit, energy harvesting, Interface circuit, piezoelectric, self-powered*

1. INTRODUCTION

Piezoelectric energy harvesting from ambient vibrations has received great attention as it can directly convert applied mechanical strain energy into useable electrical energy and can readily be integrated into microsystems [1-4]. The most important applications of piezoelectric energy harvesting devices are in wireless sensor networks (WSNs), embedded medical electronics and low power portable electronics [1,2,4-7]. In all these targeted applications, the electrical output from the energy harvesting system must be direct current (DC). This means that an interface circuit is needed to convert the alternating electrical output from the piezoelectric transducer into usable DC. Traditionally, the standard energy harvesting (SEH) interface is the most commonly used. The SEH circuit consists of a full-bridge rectifier for the AC to DC conversion [8]. The SEH interface circuit does not need any control units hence it is easier to implement compared to non-passive interfaces [9]. However, the power harvested using the SEH interface is generally limited and the interface has poor load independence [10]. DC-DC converter circuits for improved impedance matching and voltage regulation have been investigated in order to improve the output from low-power energy harvesting devices [11-14].

In order to extract more power from piezoelectric generators, nonlinear switching techniques such as synchronous switch harvesting on inductor (SSHI) and synchronous electric charge extraction (SECE) have been employed [15-17]. The synchronized switching techniques are based on the synchronized switch damping on inductor (SSDI) whereby an electrical switch (typically a combination of a digital switch and

an inductor) is employed to enable nonlinear power processing. The process artificially increases the piezoelectric transducer output voltage, resulting in a significant increase in the electrical power output [16-18]. The switching device is triggered on the maxima and minima of the displacement, and it briefly realizes the inversion of the voltage through an oscillation process. The switching device is fairly complex and is typically an externally powered microcontroller or a dedicated digital signal processing (DSP) unit which runs on external power.

Notwithstanding the many studies [15-21] which have been conducted on the SSHI techniques, most of them are limited to either theoretical simulations or to ideal cases where the switching and control circuitry is externally powered. There still remain challenges in designing efficient truly self-powered energy harvesting system. Richard et al. [22] have proposed a fully self-powered switching circuit called the electronic breaker whose typical power consumption is less than 5 % of the electrostatic energy available on the piezoelectric transducer [19,20,23]. Recently Zhu et al. [24] investigated the mechanism of the self-powered circuit breaker and also established that the electronic breaker circuit can be taken to be an efficient way for implementing self-powered piezoelectric vibration generators. In the reported power on the self-powered SSHI interfaces, the performance of the self-powered SSHI interfaces is mostly evaluated only under a specified vibrational excitation level [17-21]. The performance of these nonlinear switching interfaces relative to the SEH interfaces is hardly reported in literature. It is against this background that this paper seeks to experimentally study the energy harvesting performance of a self-powered SSHI interface circuit.

In this paper a self-powered SSHI interface circuit based on the electronic breaker circuit proposed in [24] is experimentally studied. Its performance relative to the SEH interface is studied under different vibration excitation levels. Section 2 gives an overview of the working principles of the SEH and parallel SSHI interfaces. Section 3 introduces the experimental details and procedures employed to study the self-powered SSHI circuit employing a geometrically optimized piezoelectric bimorph device. Section 4 presents results from experimental measurements. Finally Section 5 concludes the paper

2. ENERGY HARVESTING

This section presents a brief overview of the single degree of freedom (SDOF) model of an energy harvesting systems using piezoelectric materials. It also presents a brief review of the SEH where a piezoelectric device is directly connected to a bridge rectifier, and parallel SSHI interface that includes an electronic switch connected in parallel with the piezoelectric transducer

2.1 Energy Harvesting Principles

A piezoelectric energy harvesting device has the novel ability to convert mechanical vibration energy into electrical energy. The resonant piezoelectric energy harvesting device can be modeled as a single-degree-of-freedom (SDOF) spring-mass-damper system excited by a sinusoidal force at resonance (see Fig. 1). This simple model of the electromechanical system has been successfully used by previous researchers [21,25-27].

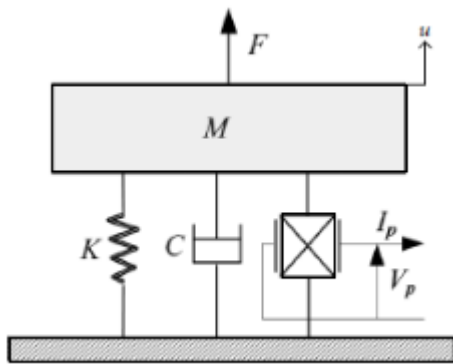


Fig. 1: A SDOF model of the energy harvesting device

The application of vibration theory together with the standard piezoelectric constitutive relations results in the following equations for the system [21,26-29]. The equation of motion for the system is given by (1) while the current flowing out of the piezoelectric transducer (I_p) is given by (2).

$$F = M\ddot{u} + C\dot{u} + Ku + \alpha V_p \quad (1)$$

$$I_p = \alpha \dot{u} - C_p \dot{V}_p \quad (2)$$

where M is the rigid mass, C is the structural damping coefficient, K is the model stiffness, F is the excitation force, u is the displacement of the rigid mass, α is the force factor of piezoelectric element, and V_p is the piezoelectric voltage.

2.2. Standard Energy Harvesting (SEH) interface.

Fig. 2 shows the architecture of the SEH interface. The typical waveforms for the SEH interface are shown in Fig. 3. Consider the case where the energy harvesting system is operating at the mechanical resonance (f) and with maximum displacement amplitude (u_m). The optimum resistance value is given by (3), and the corresponding maximum power value for the SEH is given by (4).

$$R_{opt} = \frac{1}{4fC_p} \quad (3)$$

$$(P_{SEH})_{max} = \frac{f\alpha^2 u_m^2}{C_p} \quad (4)$$

The limitation of the SEH interface is that there is no guarantee that energy flow is from the mechanical part to the electrical part. It has been observed that during a certain interval in each cycle, energy returns from the electrical part to the mechanical part, a phenomenon called “energy return”[30].

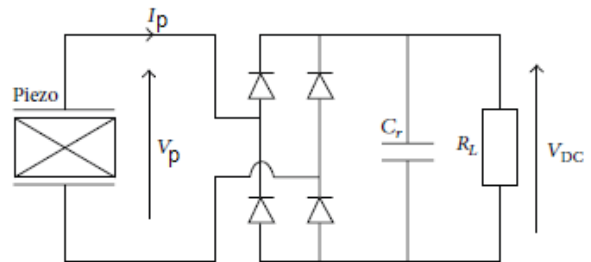


Fig. 2: Standard Interface (SEH)

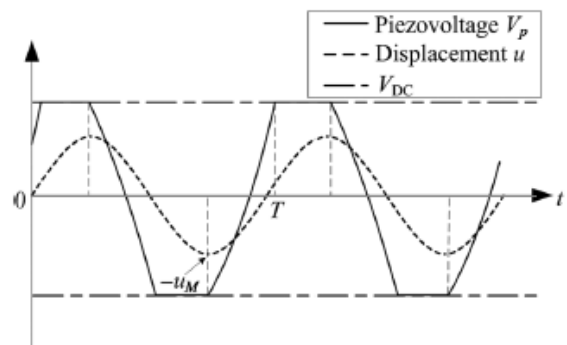


Fig. 3: Standard Interface waveforms

2.3. The Parallel Synchronised Switch Harvesting on Inductor (SSHI) Interface

The technique is implemented with a switched inductor connected in parallel with the capacitance of the piezoelectric harvesting device, as shown in Fig. 4. Theoretical waveforms for the SSHI interface are shown in Fig. 5. The maximum output power value is given by (5) for an optimal equivalent load resistor R_{opt} given by (6)

$$(P_{SSHI})_{max} = \frac{2f\alpha^2 u_m^2}{C_p} \frac{1}{1-\gamma} \tag{5}$$

$$R_{opt} = \frac{1}{2fC_p} \frac{1}{1-\gamma} \tag{6}$$

where γ is the inversion factor defined by $\gamma = e^{-\pi/(2Q)}$, with Q the quality factor of the oscillatory circuit.

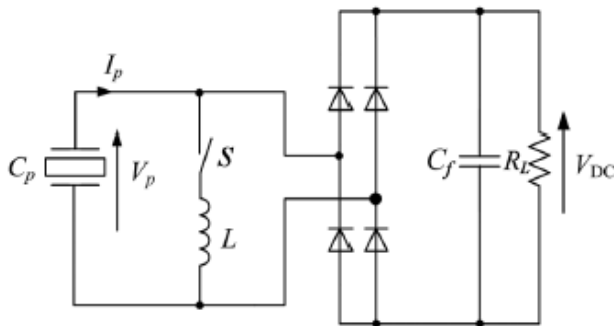


Fig. 4: SSHI Interface

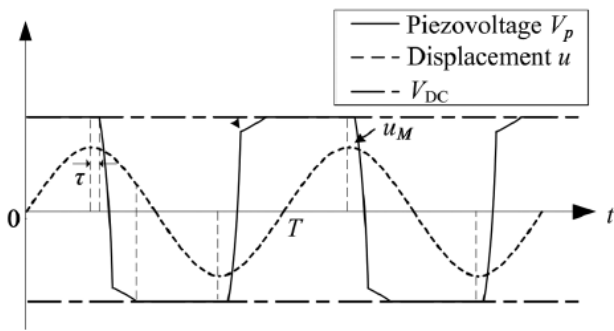


Fig. 5: Theoretical SSHI waveforms

2.4. SSHI interface and Self-Powered Issues.

The SSHI interface introduced in Section 2.3 describes an ideal interface circuit with the switching device externally powered. Thus, components for displacement peak detection and switch control are needed. In most of the reported literature on SSHI interfaces, DSPs, digital sensors and controllers employed are externally powered [15-21].

However for self-powered systems, the switching device also consumes harvested power. To implement nonlinear switching techniques with little power consumption, a self-powered switching circuit called electronic breaker was proposed by Richard et al. [22]. This self-powered electronic design (see Figure 6) has been successfully applied in the design of synchronised switching circuits by previous researchers [17,19-24]. However, it is perhaps in 2012 when Zhu et al. [25] reported on the theoretical model describing the working of the self-powered electronic breaker and also demonstrated that the electronic breaker can fulfill different switching times of the SSHI interface. Liang and Liao [23] also presented an improved analysis of the parallel SSHI self-powered interfaces and proposed an improved circuit.

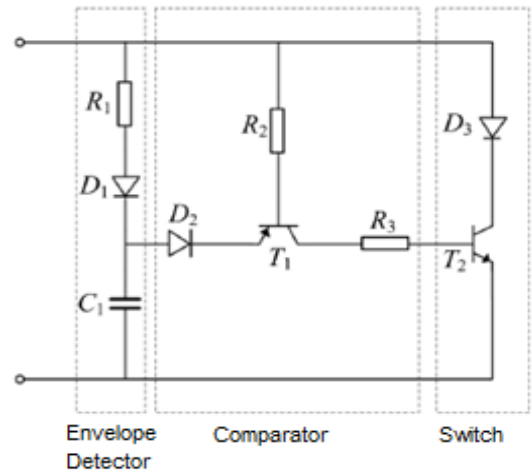


Fig. 6: Electronic breaker for switch on maximum displacement [22, 24]

The circuit in Fig. 6 consists of an envelope detector, comparator and switch. The comparator's function is to compare the piezoelectric voltage with that of the envelope voltage on capacitor C_1 . When envelope voltage is greater and the piezoelectric voltage, the PNP transistor T_1 is in non-conducting mode. When the envelope voltage is greater than the threshold voltage, T_1 is set into conducting mode. This leads to the NPN transistor T_2 being triggered on and the nonlinear processing is initiated. The electronic breaker for switch on minimum displacement operates on a similar principle only that the diodes and switching transistors are of opposite polarities. Fig. 7 shows the complete circuit implementing both the maximum and minimum circuit breakers [24]. It is this self-powered SSHI circuit which is implemented in this experimental study.

3. EXPERIMENTAL STUDY

This section presents the experimental setup and measurement procedures on the performance of the self-powered SSHI interface circuit relative to the SEH.

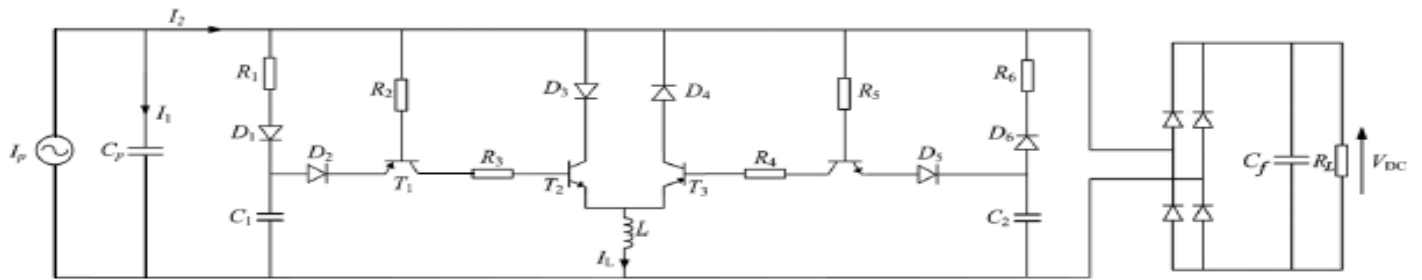


FIGURE 7: Self-powered parallel SSHI interface [24]

3.1 Experimental Setup.

A geometrically optimized piezoelectric series bimorph device with a proof mass was used as the energy harvesting transducer. The device was fabricated using two PSI-5H4E ceramic patches with nickel-plated electrodes (Piezo Systems Inc, USA) bonded to a stainless steel using conducting epoxy glue (Circuit Works, USA). The piezoelectric patches were electrically connected in series. The total device volume is about 5.5 mm³. Table 1 gives the dimensions of the piezoelectric bimorph device. The values of electrical components for the self-powered SSHI are given in Table 2.

Table 1: Dimensions of the Piezoelectric Device

	Dimensions (Thickness x Width x thickness)
Substrate (Stainless Steel)	0.120 mm x 4.0 mm x 28.25mm
Piezoelectric material (PSI-5H4E)	0.127 mm x 4.0 mm x 9.41 mm
Proof mass (lead metal)	7.000 mm x 4.0 mm x 18.83 mm

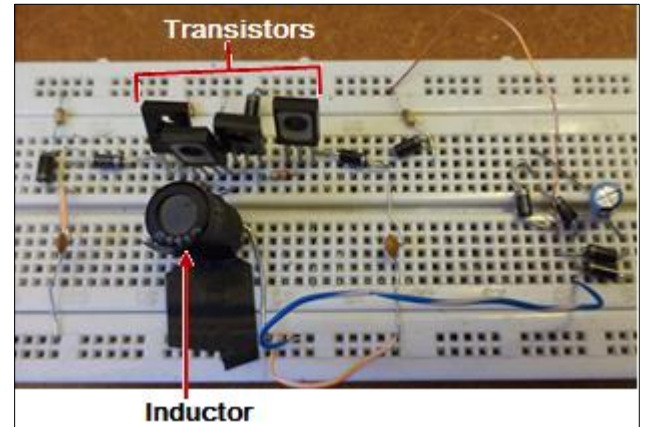


Fig. 8: Experimental Implementation of the Self-powered SSHI depicted in the schematic of Fig. 7.

Fig. 8 shows a photograph of the self-powered SSHI on breadboard. The diodes for the interface circuit chosen were the 1N4004 silicon diodes. Ideally Schottky barrier diodes (SBD) with low forward voltage drop and fast reverse recovery time could have been used. However, these SBD were outperformed by the ordinary IN4004 diodes in the preliminary investigations.

Despite the higher forward voltage drop greater than that of SBD, the IN4004 Si diodes demonstrated a superior performance because they have relatively lower reverse leakage current compared to the SBD [31]. The collector-emitter saturation voltage of the BD140 and BD139 transistors adopted in the switching circuit is 0.5V [32]. A commercially available inductor of 2 mH was used. The choice of the inductor L was such that the oscillation frequency of the LCp circuit was in the kHz region, which is much higher than the frequency of vibration of the piezoelectric generator (which was about 50 Hz). The energy consumed by the switching circuit was less than 5 % of the harvested power.

The piezoelectric bimorph device was clamped to an electromagnetic shaker, and the shaker was driven by a sinusoidal excitation signal which was generated by a function generator (Universal Test System MS9150-Metex Instruments). The ADXL202 accelerometer (Analogue Devices, USA), which has a typical sensitivity of 312 mV/g when operating from a 5 V

Table 2: Values/Specification of components for SSHI

	Component	Value/specification
Transistors	T ₁ & T ₃ (PNP) T ₂ & T ₄ (NPN)	BD 140 BD139
Capacitors	C ₁ & C ₂ C _f	330 pF 2 μF
Inductor	L	2 mH
Resistors	R ₁ & R ₆ R ₂ , R ₃ , R ₄ & R ₅	180k 3.3kΩ
Diodes	(all)	IN4004

power supply, was fixed at the clamped end to measure acceleration. The bimorph device was driven at its first-mode natural frequency of 49.87 Hz.

3.2 Experimental Procedures

With the piezoelectric transducer device driven at resonance, the output was first connected to the SEH interface. The output load resistance R_L was varied and the voltage across the resistance was measured using a digital multimeter (true rms DMM, Fluke). This procedure was repeated for the following values of excitation acceleration levels: 0.1 g, 0.2 g, 0.3 g, 0.4 g, and 0.5 g. The excitation level beyond 0.5 g amplitude was avoided to eliminate the possibility of exceeding the displacement limits and damaging the piezoelectric transducer device. Using the same test conditions, the self-powered SSHI was then connected in place of the SEH. The accelerometer output signal and the output voltage signals from the interfaces were monitored by a digital storage oscilloscope (ISOTECH-IDS-8062). The results of the experimental study are presented in Section 4.

4. EXPERIMENTAL RESULTS AND DISCUSSION

Fig. 9 shows the digital oscilloscope snapshot of the voltage waveforms observed during the experimentation with the self-powered SSHI interface. Figs. 10 and 11 show the output power as a function of load resistance for different excitation. Maximum power generated using the SEH and self- powered SSHI interfaces occur at the optimal load resistances of 1 M Ω and 6 M Ω respectively. Evidently a comparison of Fig. 10 and Fig. 11, reveals that the self-powered SSHI significantly increases the power harvested by the piezoelectric transducer relative to the SEH. The advantage of employing the self-powered SSHI over the SEH was investigated as a function of input excitation acceleration.

Fig. 12 shows a comparison of the maximum power delivered at different load resistances for the two interfaces at an excitation of 0.5 g. At the excitation, the self-powered interface shows its overwhelming superiority over the SEH interface circuit

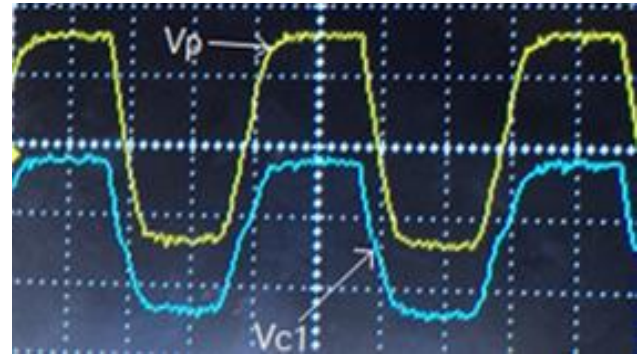


Fig. 9: CRO screen shot of the voltage waveforms of the piezoelectric transducer device (V_p) and the envelop detector (V_{c1}) of the self-powered SSHI

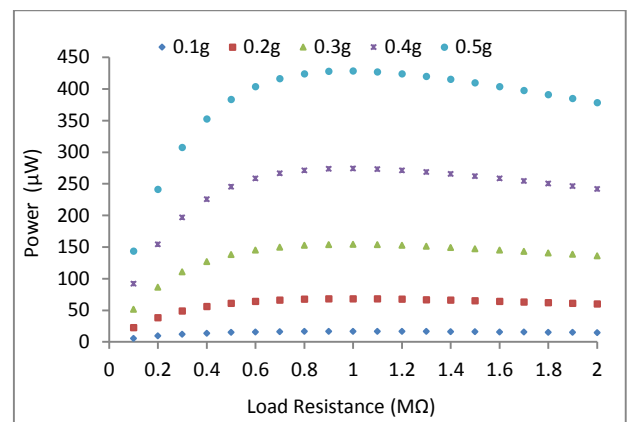


Fig. 10: Power output of SEH circuit for different excitation levels

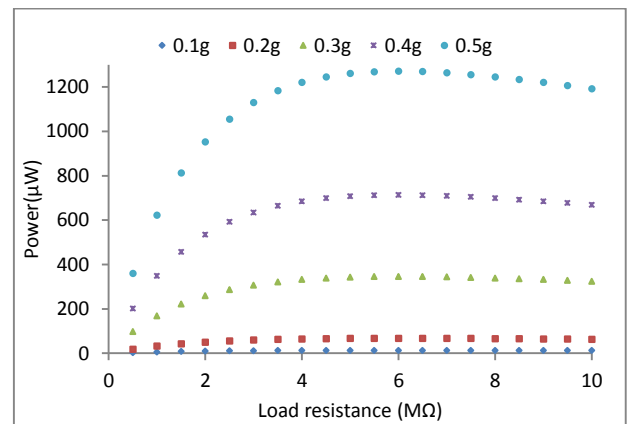


Fig. 11: Power output of self-powered SSHI interface circuit for different excitation levels

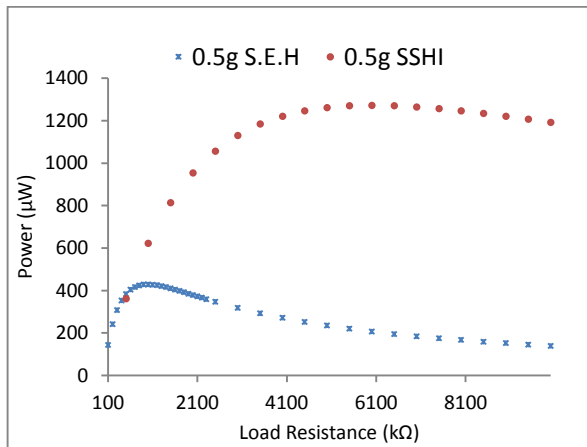


Fig. 12: Comparison of harvested power at 0.5 g

Fig. 13 shows a comparison of the maximum power delivered to the optimal load resistances for the two interfaces. From Fig. 13, the superiority of the self-powered SSHI interface over the SEH interface for excitation levels above 0.2 g is clearly evident. However, for low excitation acceleration amplitude (less than 0.2 g), the results show that the performance of the self-powered SSHI is practically not superior to the standard circuit. The explanation to this observation may be that the switching transistors employed to practically implement the SSHI

technique cannot be fully tuned on and off in time under low excitation levels [23] (in this case for less than 0.2 g).

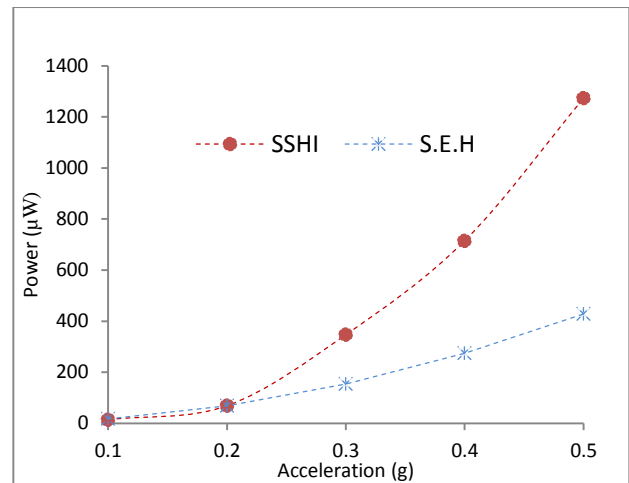


Fig. 13: Comparison of standard and SSHI performance as a function of excitation

We define the energy harvesting “enhancement” (denoted by β) as the ratio of the optimum power harvested using the self-powered SSHI to the SEH. Table 3 summarizes the power enhancement of the self-powered SSHI interface. For low excitation levels, the performance of the self-powered SSHI circuit is unexpectedly low (compared to the standard circuit and the ideal SSHI theoretical expectation). The value of β for the self-powered SSHI in this study varies as a function of the excitation level. This observation is unlike in the case of the ideal SSHI which has a constant value of β for different excitation levels. Except for the modified self-powered SSHI studied in [23], and this current study, the above observation has not been adequately reported in published literature on the piezoelectric energy harvesting using self-powered SSHI interfaces.

Table 3: Extent of enhancement as a function of excitation level

Excitation level (g)	Optimum power delivered (µW)		$\beta = P_{SSH I} / P_{standard}$
	Standard, (SEH)	SSH I	
0.1	17.13	13.86	0.8091
0.2	68.53	68.51	0.9997
0.3	154.36	346.64	2.2457
0.4	274.42	714.54	2.6038
0.5	428.76	1272.44	2.9678

5. CONCLUSION

In this paper, we have experimentally investigated the ability of the self-powered SSHI to enhance the energy harvested by a geometrically optimized piezoelectric energy harvesting device. The performance of the self-powered SSHI interface was found to depend on the input excitation levels. At acceleration levels below 0.2 g, the self-powered SSHI interface has no significant advantage over the standard energy harvesting interface. However at input acceleration beyond 0.2 g, the circuit significantly outperforms the SEH interface. Under acceleration amplitude of 0.5 g, the SEH delivered an optimum power of 428.76 μW while the self-powered SSHI interface delivered an optimum power of 1272.44 μW . This suggests that the self-powered SSHI has a gain of the order of at least 200 % for input acceleration beyond 0.5 g. The behaviour of self-powered switching interface is very much unlike ideal SSHI interface which has a constant gain over the SEH for various excitations. This phenomenon has not been widely and clearly reported except for the work by Liang and Liao [23] who studied and analysed an improved self-powered interface to SSHI technique. Thus the experimental results presented in this paper, while showing the benefits of employing synchronised techniques for harvesting energy using piezoelectric device, also exposes some design challenges that need to be further investigated.

Acknowledgment

This work was supported by the Midlands State University Research Board.

REFERENCES

- [1] H. A. Sodano, D. J. Inman, and G. Park, "A review of power harvesting from vibration using piezoelectric materials," *Shock and Vibration Digest*, vol. 36, no. 3, pp. 197–205, 2004.
- [2] G. Poulin, E. Sarraute and F. Costa, "Generation of electric energy for portable devices: comparative study of an electromagnetic and a piezoelectric system," *Sensors Actuators A*, vol. 116, no. 3, pp. 461–71, 2004.
- [3] Y. C. Shu and I. C. Lien, "Analysis of power output for piezoelectric energy harvesting systems," *Smart Materials and Structures*, vol. 15, no. 6, article 001, pp. 1499–1512, 2006.
- [4] S. Roundy, P. K. Wright, and J. M. Rabaey, *Energy Scavenging For Wireless Sensor Networks: With Special Focus on Vibrations*, Technology and Engineering, Springer, 2004.
- [5] J. A. Paradiso and T. Starner, "Energy scavenging for mobile and wireless electronics," *IEEE Pervasive Computing*, vol. 4, no. 1, pp. 18–27, 2005.
- [6] S. R. Anton and H. A. Sodano, "A review of power harvesting using piezoelectric materials (2003–2006)," *Smart Material and Structures*, vol.16, no. 3, pp. R1–21, 2007.
- [7] A. Nechibvute, A. Chawanda, and P. Luhanga, "Piezoelectric Energy Harvesting Devices: An Alternative Energy Source for Wireless Sensors," *Smart Materials Research*, vol. 2012, Article ID 853481, 13 pages, 2012. doi:10.1155/2012/853481
- [8] R D'hulst, T. Sterken, R.Puers, G. Deconinck, G. and J. Driesen, "Power processing circuits for piezoelectric vibration-based energy harvesters," *IEEE Transactions on Industrial Electronics*, vol. 57, no.12, pp. 4170-4177, 2010.
- [9] J. Liang and W.-H. Liao, "Energy flow in piezoelectric energy harvesting systems," *Smart Materials and Structures Journal*, vol. 20, no. 1, 2011.
- [10] Y. Wu, A. Badel, F. Formosa, W. Liu and A. E. Agbossou; "Piezoelectric vibration energy harvesting by optimized synchronous electric charge extraction," *Journal of Intelligent Material Systems and Structures* vol. 24, no.12, pp. 1445-1458, 2012.
- [11] G. K. Ottman, H. F. Hofmann, A.C. Bhatt, and G. A. Lesieutre, "Adaptive piezoelectric energy harvesting circuit for wireless remote power supply," *IEEE Transactions on Power Electronics*, vol. 17, no. 5, pp. 669–676, 2002.
- [12] G. K. Ottman, H. F. Hofmann, and G. A. Lesieutre, "Optimized piezoelectric energy harvesting circuit using step-down converter in discontinuous conduction mode," *IEEE Transactions on Power Electronics*, vol. 18, no. 2, pp. 696–703, 2003.
- [13] K. Hyeoungwoo, S. Priya, H. Stephanou, K. Uchino, "Consideration of Impedance Matching Techniques for Efficient Piezoelectric Energy Harvesting," *IEEE Transactions on Ultrasonics, Ferroelectrics and Frequency Control*, vol. 54, no. 9, pp. 1851-1859, 2007.
- [14] Y. Ramadass and A. Chandrakasan, "An efficient piezoelectric energy harvesting interface circuit using a bias-

- flip rectifier and shared inductor,” *IEEE Journal of Solid-State Circuits*, vol. 45, no. 1, pp. 189–204, 2010.
- [15] K. Makihara, J. Onoda, and T. Miyakawa, “Low energy dissipation electric circuit for energy harvesting,” *Smart Materials and Structures*, vol. 15, no. 5, pp. 1493–1498, 2006.
- [16] A. Badel, D. Guyomar, E. Lefeuvre, C. Richard, “Piezoelectric energy harvesting using a synchronized switch technique,” *Journal of Intelligent Material Systems and Structures*, vol. 17 no. 8-9, pp. 831-839, 2006.
- [17] D. Guyomar, A. Badel, E. Lefeuvre, and C. Richard, “Toward energy harvesting using active materials and conversion improvement by nonlinear processing,” *IEEE Transactions on Ultrasonics, Ferroelectrics, and Frequency Control*, vol. 52, no. 4, pp. 584–594, 2005.
- [18] E. Lefeuvre, A. Badel, C. Richard, D. Guyomar, “Piezoelectric energy harvesting device optimization by synchronous electric charge extraction,” *Journal of Intelligent Material Systems and Structures*, vol.16, no.10, pp. 865-876, 2005.
- [19] M. Lallart, and D. Guyomar, “An optimized self-powered switching circuit for non-linear energy harvesting with low voltage output,” *Smart Materials and Structures*, vol. 17, no. 3, 035030, 2008.
- [20] M. Lallart, E. Lefeuvre, C. Richard and D. Guyomar, “Self-powered circuit for broadband, multimodal piezoelectric vibration control,” *Sensors and Actuators A*, vol.143, no.2, pp. 377-382, 2008.
- [21] E. Lefeuvre, A. Badel, C. Richard, L. Petit, and D. Guyomar, “A comparison between several vibration-powered piezoelectric generators for standalone systems,” *Sensors and Actuators A*, vol. 126, no. 2, pp. 405–416, 2006.
- [22] C. Richard, D. Guyomar and E. Lefeuvre, “Self-powered electronic breaker with automatic switching by detecting maxima or minima of potential difference between its power electrodes,” *Patent PCT/FR2005/003000* (publication number: WO/2007/063194), 2007.
- [23] J. Liang and W. H. Liao, “Improved design and analysis of self-powered synchronized switch interface circuit for piezoelectric energy harvesting systems,” *IEEE Transactions on Industrial Electronics*, vol. 59, no.4, pp. 1950-1960, 2012.
- [24] L. Zhu, R. Chen and X. Liu, “Theoretical analyses of the electronic breaker switching method for nonlinear energy harvesting,” *Journal of Intelligent Material Systems and Structures*, vol. 23, no. 4, pp. 441–451, 2012.
- [25] E. Halvorsen, “Energy harvesters driven by broadband random vibrations,” *Journal of Microelectromechanical Systems*, vol. 17, no. 5, pp. 1061–1071, 2008.
- [26] N. G. Stephen, “On energy harvesting from ambient vibration,” *Journal of Sound and Vibration*, vol. 293, no. 1-2, pp. 409–425, 2006.
- [27] F. Lu, H. P. Lee, and S. P. Lim, “Modeling and analysis of micro piezoelectric power generators for micro-electromechanical systems applications,” *Smart Materials and Structures*, vol. 13, no. 1, pp. 57–63, 2004.
- [28] L. Tang, Y. Yang, Y. K. Tan, and S. K. Panda, “Applicability of synchronized charge extraction technique for piezoelectric energy harvesting,” in *Active and Passive Smart Structures and Integrated Systems*, vol. 7977 of *Proceedings of SPIE*, San Diego, Calif, USA, March 2011.
- [29] L.-C. J. Blystad, E. Halvorsen, and S. Husa, “Piezoelectric MEMS energy harvesting systems driven by harmonic and random vibrations,” *IEEE Transactions on Ultrasonics, Ferroelectrics, and Frequency Control*, vol. 57, no. 4, pp. 908–919, 2010.
- [30] J. R. Liang and W. H. Liao, “Piezoelectric energy harvesting and dissipation on structural damping,” *Journal of Intelligent Material Systems and Structures*, vol. 20, no. 5, pp. 515–527, Mar. 2009.
- [31] E. L. Worthington, “Piezoelectric energy harvesting: Enhancing power output by device optimisation and circuit techniques,” *PhD Thesis*, Cranfield University, pp. 214-221, 2010.
- [32] “BD139, BD140 Datasheet,” ST Semiconductor, <http://www.st.com/web/en/resource/technical/document/datasheet/CD00001225.pdf>; (accessed August 2013).